Available online at www.sciencedirect.com

ScienceDirect

Procedia Engineering 114 (2015) 102 – 109

Procedia Engineering

www.elsevier.com/locate/procedia

1st International Conference on Structural Integrity

Comparative evaluation of single-lap joints bonded with different adhesives by cohesive zone modelling

R.D.S.G. Campilho[a,]*, T.A.B. Fernandes[a]

[a]*Departamento de Engenharia Mecânica, Instituto Superior de Engenharia do Porto, Instituto Politécnico do Porto, Rua Dr. António Bernardino de Almeida, 431, 4200-072 Porto, Portugal.*

Abstract

Structures built from several components require some means of joining. In this context, bonding with adhesives has several advantages compared to traditional joining methods, e.g. reduction of stress concentrations, reduced weight penalty and easy manufacturing. Adhesives can be strong and brittle (e.g., Araldite® AV138) or less strong and ductile (e.g., Araldite® 2015). A new family of polyurethane adhesives combines high strength and ductility (e.g., Sikaforce® 7888). In this work, the performance of the three above mentioned adhesives was tested in single-lap joints with varying values of overlap length (L_O). The experimental work carried out is accompanied by a detailed numerical analysis by Finite Elements, based on Cohesive Zone Models (CZM). This procedure enabled detailing the performance of this predictive technique applied to bonded joints. Moreover, it was possible to evaluate which family of adhesives is more suited for each joint geometry. CZM revealed to be highly accurate, except for largely ductile adhesives, although this could be circumvented with a different cohesive law.

Peer-review under responsibility of INEGI - Institute of Science and Innovation in Mechanical and Industrial Engineering

Keywords: Epoxy/epoxides; polyurethane; finite element analysis; fracture mechanics; aluminium and alloys.

1. Introduction

Adhesive-bonding is often used in multi-component structures, since it provides several advantages over welding, riveting and bolting methods, such as reduction of stress concentrations, reduced weight penalty and easy manufacturing. Commercial structural adhesives range from strong and brittle to less strong and ductile. A new

* Corresponding author. Tel.: +351 939526892; fax: +351 228321159.
E-mail address: raulcampilho@gmail.com

Peer-review under responsibility of INEGI - Institute of Science and Innovation in Mechanical and Industrial Engineering
doi:10.1016/j.proeng.2015.08.047

family of polyurethane adhesives combines high strength with large ductility [1]. The main parameters affecting the joints' strength are L_O, adherend material (i.e., Young's modulus, E) and thickness, and adhesive thickness (t_A) and properties (mainly strength and ductility). The effect of L_O depends on the type of adhesive (i.e. ductile or brittle) and on the type of adherend [2]. For bonded joints with elastic adherends and ductile adhesives, the strength is roughly proportional to L_O. For joints with elastic adherends and brittle adhesives, the joint strength is not proportional to the overlap and a limit strength is attained, because the adhesive does not accommodate peak stresses and failure is ruled by these peaks. In joints with yielding adherends, failure is ruled by the adherend yielding and again a steady-state value is attained in the maximum load (P_m) vs. L_O plot [3]. The adherend properties (stiffness, strength and ductility) also have a large effect on the joints' strength. The higher the adherend stiffness is, the smaller are the strains at the overlap edges, and lower will become the effect of the differential straining in the adhesive, i.e., the shear stress distribution becomes more flat [4]. Excessive adherend yielding at the bonding edges can trigger premature joint failure because large plastic strains appear at these regions [5]. The effect of t_A on single-lap joints is well documented. Most of the results are for epoxy adhesives and show that the lap joint strength decreases with the increase of t_A [6]. The adhesive properties have a high influence on the joint strength, but a stronger adhesive does not necessarily give a higher joint strength. A high strength but brittle adhesive achieves locally high stresses in the overlap corners, but does not allow stress redistributions to the low stressed areas. As a result, the average shear stress at failure is very low [7]. On the other hand, adhesives with high ductility and low modulus have generally a low strength. However, they distribute the stresses more uniformly along the bondline and deform plastically, which turns the joints stronger than with strong but brittle adhesives [8].

Currently, a large number of predictive techniques is available for bonded joints, either analytical or numerical. Extensive reviews of these methods are provided by da Silva et al. [9] for analytical methods and He [10] for Finite Element-based techniques. Analytical methods are easy to use, but they usually consider simplification assumptions [11]. For complex geometries and elaborate material models, a Finite Element analysis is preferable to obtain the stress distributions. Fracture mechanics-based methods use the fracture toughness of materials as the leading parameter for fracture assessment [12]. More recently, powerful numerical techniques such as CZM became available, which predict the structures' strength by combining stress criteria to account for damage initiation with energetic, e.g. fracture toughness, data to estimate crack propagation [13], [14]. This technique is particularly attractive for bonded joints, since the ductility plays a major role in the failure process because of the stress gradients. However, the method relies on an accurate measurement of the cohesive strengths in tension and shear (t_n^0 and t_s^0, respectively), and of the tensile (G_{IC}) and shear toughness (G_{IIC}) [15]. CZM accurately predicts the strength of bonded joints if the fracture laws are estimated correctly [16]. Ridha et al. [17] studied by CZM adhesively-bonded scarf repairs on composite panels bonded with a ductile epoxy adhesive. Softening laws with linear, exponential and trapezoidal shapes were compared. The predictions were very accurate, although the linear and exponential models resulted in under predictions of the repairs strength of nearly 20%, on account of excessive plastic degradation at the bond edges that was not observed in the real joints.

In this work, the performance of a brittle (Araldite® AV138), a moderately ductile (Araldite® 2015) and a largely ductile adhesive (Sikaforce® 7888) was tested in single-lap joints between aluminium adherends with varying values of L_O. The experimental work carried out is accompanied by a detailed analysis by Finite Elements, starting with the plot of elastic stress distributions, and strength prediction based on CZM. This procedure enabled assessing in detail the performance of the predictive technique applied to bonded joints. Moreover, it was possible to evaluate which family of adhesives is more suited for each joint geometry.

2. Experiments

2.1. Materials

The adherends were cut from a high strength aluminium alloy sheet (AA6082 T651) by precision disc cutting. This material was characterized in bulk tension in a previous work by the authors [18] using dogbone specimens and the following mechanical properties were obtained: E of 70.07 ± 0.83 GPa, tensile yield stress (σ_y) of 261.67 ± 7.65

MPa, tensile failure strength (σ_f) of 324 ± 0.16 MPa and tensile failure strain (ε_f) of 21.70 ± 4.24%. The experimental curves and the numerical approximation, to be used further in work, are presented in Fig. 1.

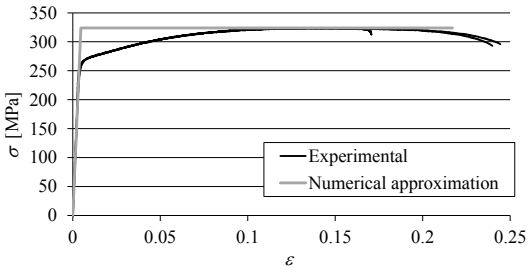

Fig. 1: σ-ε curves of the aluminium: experimental data and numerical approximation.

Three structural adhesives, ranging from brittle to highly ductile, were considered: the brittle epoxy Araldite® AV138, the ductile epoxy Araldite® 2015 and the high strength and ductile polyurethane Sikaforce® 7888. The mechanical and toughness properties of these adhesives were obtained in previous works by the authors by experimental testing [2], [7], [19]. Bulk specimens were tested in a servo-hydraulic machine to obtain E, σ_f and ε_f. The DCB test was selected to obtain G_{IC} and the End-Notched Flexure (ENF) test was used for G_{IIC}. The collected data of the adhesives is summarized in Table 1.

Table 1: Properties of the adhesives Araldite® AV138, Araldite® 2015 and SikaForce® 7888 [2], [7], [19]

Property	**AV138**	**2015**	**7888**
Young's modulus, E [GPa]	4.89±0.81	1.85±0.21	1.89±0.81
Poisson's ratio, ν	0.35 *	0.33 *	0.33 *
Tensile yield strength, σ_y [MPa]	36.49±2.47	12.63±0.61	13.20±4.83
Tensile failure strength, σ_f [MPa]	39.45±3.18	21.63±1.61	28.60±2.0
Tensile failure strain, ε_f [%]	1.21±0.10	4.77±0.15	43.0±0.6
Shear modulus, G [GPa]	1.56±0.01	0.56±0.21	0.71 [b]
Shear yield strength, τ_y [MPa]	25.1±0.33	14.6±1.3	-
Shear failure strength, τ_f [MPa]	30.2±0.40	17.9±1.8	20 *
Shear failure strain, γ_f [%]	7.8±0.7	43.9±3.4	100 *
Toughness in tension, G_{IC} [N/mm]	0.20 [a]	0.43±0.02	1.18±0.22
Toughness in shear, G_{IIC} [N/mm]	0.38 [a]	4.70±0.34	8.72±1.22

* manufacturer's data

[a] estimated in reference [18], [b] estimated from Hooke's law

2.2. Joint configurations

The geometry and dimensions of the single-lap joints are described in Fig. 2. The joint dimensions are: plate thickness t_P = 3 mm, t_A = 0.2 mm, L_O = 12.5, 25, 37.5 and 50 mm, and joint total length between grips L_T = 180 mm.

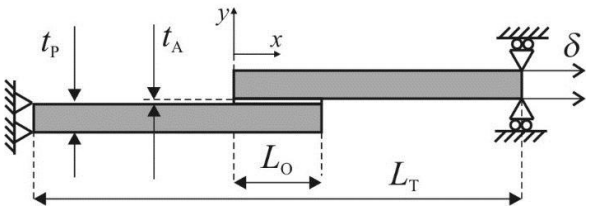

Fig. 2: Geometry of the single-lap joints used in the present work.

The bonding process was preceded by grit blasting with corundum sand, debris cleaning with acetone and assembly in a steel mould for the correct alignment between the adherends. Curing of the specimens was carried out according to the manufacturer's specifications for complete curing, i.e. for at least 48 hours at room temperature. The specimens were tested in a Shimadzu AG-X 100 testing machine with a 100 kN load cell, at room temperature and under displacement control (1 mm/min). Four valid results were always provided for each condition.

3. Numerical modelling

The FEM software ABAQUS® was selected to perform the numerical analysis, which has a CZM embedded module, to predict the strength of the single-lap joints. An initial stress analysis was performed to better understand the observed behaviour. The adherends were modelled as elasto-plastic solids with an approximated curve to the real σ-ε curve of the aluminium (Fig. 1). The adhesive was modelled with CZM elements. Geometrical non-linearities were considered. The joints were modelled as two-dimensional, with plane-strain solid elements (CPE4 from ABAQUS®). Different mesh refinements were considered for the stress and failure analyses (Fig. 3 shows a representative mesh for the failure analysis by CZM).

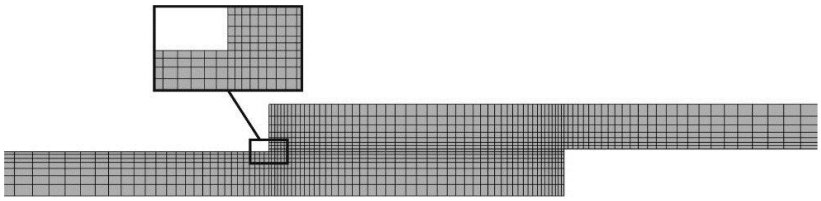

Fig. 3: Mesh for the CZM analysis (L_O=12.5 mm).

In both scenarios, the meshes were constructed with bias effects from the adhesive centre regions towards the overlap edges, and towards the adhesive layer in the joint thickness direction, to reduce the computational effort but without compromising the precision of the results. The meshes for the stress analysis models are highly refined, with 0.02 mm × 0.02 mm elements in the adhesive layer, to accurately capture the peak stresses at the overlap ends, which theoretically are singular regions [20]. For the CZM failure analyses, only one element was considered in the adhesive thickness direction. Thus, the element size in the adhesive was 0.2 mm × 0.2 mm. The number of elements in the adherends' thickness direction was 30, while for the adhesive length between 30 and 120 elements were used (from the smallest to the biggest value of L_O). Restraining and loading conditions were introduced to faithfully model the real testing conditions, consisting on clamping of the joint at one edge and applying a vertical restraint and tensile displacement at the opposite edge. In the CZM analysis, the adhesive was modelled by the continuum approach, with a single row of cohesive elements and a traction-separation law including the adhesive layer stiffness.

3.1. CZM model description

CZM are based on a relationship between stresses and relative displacements connecting initially superimposed nodes of the cohesive elements (Fig. 4), to simulate the elastic behaviour up to a peak load and subsequent softening, to model the gradual degradation of material properties up to complete failure. The areas under the traction-separation laws in each mode of loading (tension and shear) are equalled to the respective fracture energy. Under pure mode, damage propagation occurs at a specific integration point when the stresses are released in the respective traction-separation law. Under mixed mode, energetic criterions are often used to combine tension and shear [17]. The traction-separation law assumes an initial linear elastic behaviour followed by linear evolution of damage. The elastic behaviour of the cohesive elements up to the tipping tractions is defined by an elastic constitutive matrix relating stresses and strains across the interface, containing E and the shear modulus (G) as main parameters. Damage initiation under mixed-mode can be specified by different criteria. In this work, the quadratic nominal stress criterion was considered for the initiation of damage. After the peak value in Fig. 4 is attained (t_m^0), the material

stiffness is degraded. Complete separation is predicted by a linear power law form of the required energies for failure in the pure modes. For full details of the presented model, the reader can refer to reference [15].

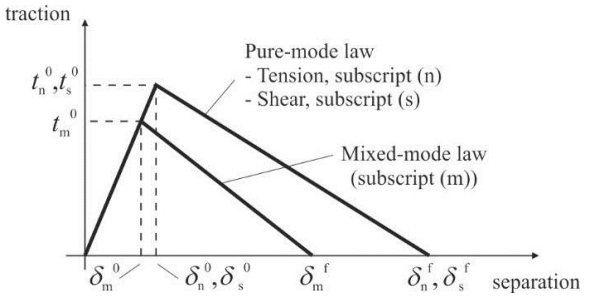

Fig. 4: Linear CZM law: pure and mixed-mode laws.

Table 2 shows the values introduced in ABAQUS® for the simulation of damage growth in the adhesive layer. These properties were estimated from the data of Table 1, considering the average values of σ_f and τ_f from the characterization tests to define t_n^0 and t_s^0, respectively.

Table 2: Cohesive parameters of the adhesives Araldite® AV138, Araldite® 2015 and SikaForce® 7888

Property	AV138	2015	7888
E [GPa]	4.89	1.85	1.89
G [GPa]	1.56	0.56	0.71
t_n^0 [MPa]	39.45	21.63	28.60
t_s^0 [MPa]	30.2	17.9	20
G_{IC} [N/mm]	0.20	0.43	1.18
G_{IIC} [N/mm]	0.38	4.70	8.72

4. Results

4.1. Fracture modes

After performing the experimental tests, all failures were cohesive in the adhesive layer. However, plastic deformation was found in the adherends for some of the test conditions, namely for the conditions with bigger failure loads. All load-displacement (P-δ) curves were predominantly linear up to failure, except for the L_O=50 mm joints bonded with the Sikaforce® 7888. This behaviour was consistent with the numerical results.

4.2. Bondline stresses

A peel (σ_y) and shear (τ_{xy}) stress analysis is carried out at the adhesive mid-thickness that enables further discussions on the obtained strength results. The plots of σ_y and τ_{xy} stress distributions in the adhesive layer as a function of percentile L_O are presented in Fig. 5 and Fig. 6, respectively. A normalization procedure was carried out, dividing σ_y and τ_{xy} stresses by τ_{avg}, the average shear stress along the overlap for the respective value of L_O. An identical normalization procedure was carried out for L_O by plotting stresses vs. x/L_O ($0 \leq x \leq L_O$). The results are relative to the joints bonded with the Araldite® 2015 and they are representative of all joints.

σ_y stresses are typically much lower in magnitude than τ_{xy} stresses, except at the bond edges, in which σ_y stress singularities build up owing to the square-edge geometry [21], [22]. At the inner overlap region, these stresses are compressive. The peak peel stresses at the bond edges increase with L_O, and these are responsible for a significant strength reduction of bonded joints [20], [23].

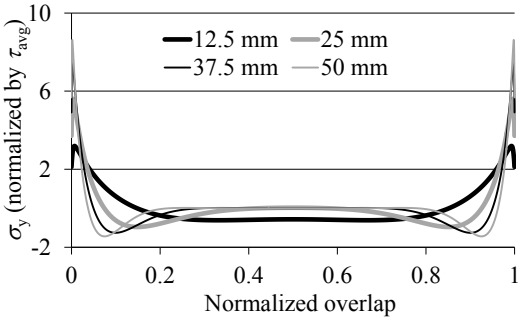

Fig. 5: σ_y stresses as a function of L_O.

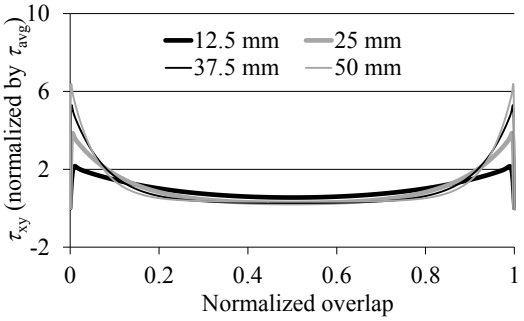

Fig. 6: τ_{xy} stresses as a function of L_O.

The obtained τ_{xy} distributions are also consistent with the available literature results, with a smaller load bearing potential at the overlap inner region and peaking towards the overlap edges [24], [25]. τ_{xy} stress gradients increase with L_O because of the increasing gradient of longitudinal strains in the adherends caused by the bigger bonding areas and loads. This markedly affects the strength improvement of bonded joints for brittle adhesives, which do not allow plasticization at the overlap edges. Oppositely, ductile adhesives enable the redistribution of stresses while the inner region of the overlap is gradually put under loads, giving a bigger increase of the joint strength [20], [26].

4.3. Strength prediction

In the CZM analysis the adhesive layer was modelled by a single row of cohesive elements, i.e. by the continuum approach, and the adherends were considered as elasto-plastic using the properties defined in Section 2.1.

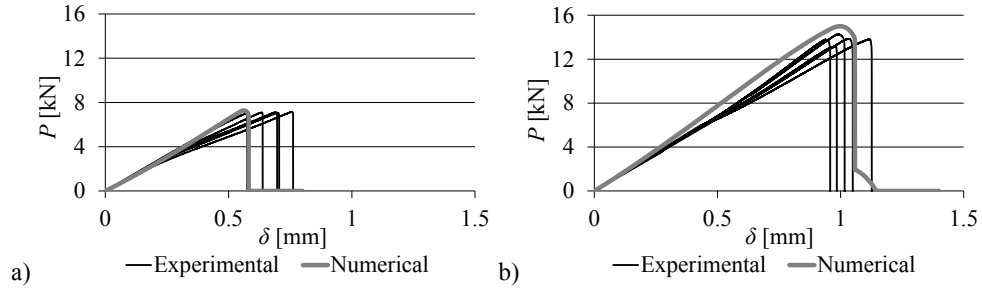

Fig. 7: Experimental and CZM P-δ curves for the L_O=25 mm Araldite® AV138 (a) and L_O=50 mm Araldite® 2015 (b) joints.

Fig. 7 gives an example of the overall correlation obtained between the experimental and numerical (CZM) P-δ curves, by showing as an example L_O=25 mm Araldite® AV138 (a) and L_O=50 mm Araldite® 2015 joints (b). For the Sikaforce® 7888, the numerical results under predict the experiments, but this will be specifically addressed further in this paper. Fig. 8 gives the summarized results of P_m-L_O for the three adhesives, considering the experimental values of average and respective error bars, and also the numerical predictions by CZM (dots with deviation and lines, respectively). The experimental results show a distinct behavior between the three bonded systems, which is highly dependent on the adhesive properties (stiffness, strength and ductility). The adhesive stiffness has a large effect on stress distributions: a low stiffness adhesive provides a more uniform stress distribution compared to a stiff adhesive [2], which puts the Araldite® AV138 in disadvantage in view of the values of E presented in Table 1. The adhesive strength has more preponderance for short overlaps, in which σ_y and τ_{xy} stresses are more even along the overlap (Fig. 5 and Fig. 6). A ductile adhesive is able to redistribute the load and make use of the less stressed parts of the overlap, whereas a brittle adhesive concentrates the load at the ends of the overlap without giving the possibility of plasticization, giving a low average shear stress at failure [6]. In view of this, the Araldite® AV138, which is a very strong but brittle adhesive, performs slightly better than the Araldite® 2015 (less strong but ductile) for short overlaps. However, by increasing L_O, the Araldite® 2015 quickly surpasses the Araldite® AV138 because it is moderately ductile and, thus, it is able to sustain some plasticity before failure, unlike the Araldite® AV138. Fig. 8 shows a marked change between L_O=12.5 and 25 mm, in which the limited plasticity of the Araldite® 2015 is used, and a more moderate deviation from this point on. Compared with these two adhesives, the Sikaforce® 7888 is simultaneously strong and highly ductile, in such a way that failure with this adhesive approaches the conditions of generalized failure up to substantially long overlaps [26]. Thus, compared to the Araldite® 2015 and the Araldite® AV138, it excels in P_m values from small to large values of L_O. In view of these results, recommendation goes to using less strong but ductile adhesives (if it is not possible to combine both features), except for very small overlaps, in which strong adhesives also perform well. Adhesives that combine these two characteristic are undoubtedly the best choice.

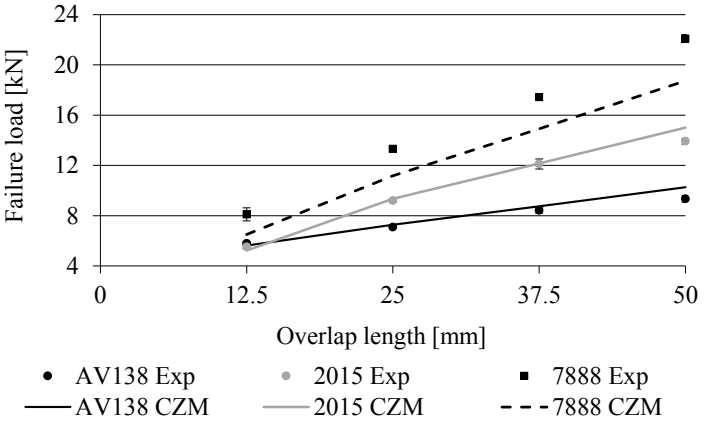

Fig. 8: Experimental and CZM values of P_m as a function of L_O.

5. Conclusions

This work aimed at providing advanced numerical tools for adhesive selection to be applied in single-lap joints between aluminium adherends with varying values of L_O. Three adhesives, ranging from brittle to largely ductile, were considered to evaluate two numerical methods at opposing failure conditions. The CZM technique was considered for strength prediction. The experimental analysis revealed a distinct behaviour between the adhesives: (1) the brittle adhesive showed a small improvement of P_m with L_O because of the lack of plasticization at the damage initiation sites, (2) the moderately ductile adhesive showed a smaller value of P_m for the smallest L_O, but was able to sustain plasticization at the overlap edges, and thus to increase strength at a higher rate than the former

brittle adhesive, and finally, (3) the high strength and high ductility polyurethane showed the highest strength and improvement rate of P_m on account of failure under conditions approaching generalised failure of the adhesive. The Finite Element stress analysis enabled the detailed justification of this behaviour. CZM modelling with triangular shape damage laws revealed to be highly accurate for the brittle and moderately ductile adhesives, while underestimating by a non-negligible amount P_m for the polyurethane (maximum of 19.7%). A mesh dependency study confirmed that this numerical tool is highly stable to the mesh size. As a result of this work, it was possible to evaluate in detail CZM modelling for strength prediction and provide an indication of the behaviour of different types of adhesives applied to single-lap joints.

References

[1] R.D.S.G. Campilho, D.C. Moura, D.J.S. Gonçalves, J.F.M.G. da Silva, M.D. Banea, L.F.M. da Silva, Fracture toughness determination of adhesive and co-cured joints in natural fibre composites, Compos.: Part B – Eng. 50 (2013) 120-126.

[2] R.D. Adams, J.C. Comyn, W.C. Wake, Structural adhesive joints in engineering, 2nd ed., Chapman & Hall, London, 1997.

[3] M.S. Kafkalidis, M.D. Thouless, The effects of geometry and material properties on the fracture of single lap-shear joints, Int. J. Solids Struct. 39 (2002) 4367-4383.

[4] O. Volkersen, Die nietkraftoerteilung in zubeanspruchten nietverbindungen mit konstanten loschonquerschnitten, Luftfahrtforschung 15 (1938) 41-47.

[5] B. Haghpanah, S. Chiu, A. Vaziri, Adhesively bonded lap joints with extreme interface geometry, Int. J. Adhes. Adhes. 48 (2014) 130-138.

[6] R.D. Adams, N.A. Peppiatt, Stress analysis of adhesive-bonded lap joints, J. Strain Anal. 9 (1974) 185-196.

[7] R.D.S.G. Campilho, M.D. Banea, J.A.B.P. Neto, L.F.M. da Silva, Modelling adhesive joints with cohesive zone models: effect of the cohesive law shape of the adhesive layer, Int. J. Adhes. Adhes. 44 (2013) 48-56.

[8] R.D.S.G. Campilho, A.M.G. Pinto, M.D. Banea, R.F. Silva, L.F.M. da Silva, Strength improvement of adhesively-bonded joints using a reverse-bent geometry, J. Adhes. Sci. Technol. 25 (2011) 2351-2368.

[9] L.F.M. da Silva, P.J.C. das Neves, R.D. Adams, J.K. Spelt, Analytical models of adhesively bonded joints – Part I: Literature survey, Int. J. Adhes. Adhes. 29 (2009) 319-330.

[10] X. He, A review of finite element analysis of adhesively bonded joints, Int. J. Adhes. Adhes. 31 (2011) 248-264.

[11] L.J. Hart-Smith, Adhesive bonded single lap joints, NASA Contractor Report 112235, 1973.

[12] H. Chai, Shear fracture, Int. J. Fract. 37 (1988) 137-159.

[13] R.D.S.G. Campilho, M.F.S.F. de Moura, A.M.J.P. Barreto, J.J.L. Morais, J.J.M.S. Domingues, Fracture behaviour of damaged wood beams repaired with an adhesively-bonded composite patch, Compos.: Part A – Appl. Sci. 40 (2009) 852-859.

[14] P.B. Woelke, M.D. Shields, N.N. Abboud, J.W. Hutchinson, Simulations of ductile fracture in an idealized ship grounding scenario using phenomelogical damage and cohesive zone models, Comput. Mater. Sci, 80 (2013) 79-95.

[15] R.D.S.G. Campilho, M.D. Banea, J.A.B.P. Neto, L.F.M. da Silva, Modelling of single-lap joints using cohesive zone models: effect of the cohesive parameters on the output of the simulations, J. Adhesion 88 (2012) 513-533.

[16] R.D.S.G. Campilho, M.F.S.F. de Moura, D.A. Ramantani, J.J.L. Morais, J.J.M.S. Domingues, Buckling behaviour of carbon-epoxy adhesively-bonded scarf repairs, J. Adhes. Sci. Technol. 23 (2009) 1493-1513.

[17] M. Ridha, V.B.C. Tan, T.E. Tay, Traction-separation laws for progressive failure of a bonded scarf repair of composite panel, Compos. Struct. 93 (2010) 1239-1245.

[18] R.D.S.G. Campilho, M.D. Banea, A.M.G. Pinto, L.F.M. da Silva, A.M.P. de Jesus, Strength prediction of single- and double-lap joints by standard and extended finite element modeling, Int. J. Adhes. Adhes. 31 (2011) 363-372.

[19] J.A.B.P. Neto, R.D.S.G. Campilho, L.F.M. da Silva, Parametric study of adhesive joints with composites, Int. J. Adhes. Adhes. 37 (2012) 96-101.

[20] R.D.S.G. Campilho, M.F.S.F. de Moura, J.J.M.S. Domingues, Modelling single and double-lap repairs on composite materials, Compos. Sci. Technol. 65 (2005) 1948-1958.

[21] J. Radice, J. Vinson, On the use of quasi-dynamic modeling for composite material structures: analysis of adhesively bonded joints with midplane asymmetry and transverse shear deformation, Compos. Sci. Technol. 66 (2006) 2528-2547.

[22] A.A. Taib, R. Boukhili, S. Achiou, H. Boukehili, Bonded joints with composite adherends. Part II. Finite element analysis of joggle lap joints, Int. J. Adhes. Adhes. 26 (2006) 237-248.

[23] R.D.S.G. Campilho, M.F.S.F. de Moura, J.J.M.S. Domingues, Numerical prediction on the tensile residual strength of repaired CFRP under different geometric changes, Int. J. Adhes. Adhes. 29 (2009) 195-205.

[24] M. Vable, J.R. Maddi, Boundary element analysis of adhesively bonded joints, Int. J. Adhes. Adhes. 26 (2006) 133-144.

[25] Q. Luo, L. Tong, Fully-coupled nonlinear analysis of single lap adhesive joints, Int. J. Solids Struct. 44 (2007) 2349-2370.

[26] M. Davis, D. Bond, Principles and practices of adhesive bonded structural joints and repairs, Int. J. Adhes. Adhes. 19 (1999) 91-105.